**Quarterly Report** to the
Office of Pipeline Safety, US Dept. of Transportation
Interagency Agreement DTRS56-04-X-0025
April 30, 2004 as Modified August 4, 2004

**Task Order #02**
**Fatigue Fracture and Crack Arrest in High-Strength Pipeline Steels**
For the Quarter ending
**October 31, 2005**

1. **Progress, Findings, and Activities:**
   a) Task 1 Standards - Awaiting data on which to act

   b) Task 2 Fatigue and Fracture – As a precursor to the fatigue work, standard tensile testing was conducted on the pipe sections supplied to us by a pipeline operator. Data from that part of this project is supplied in the attached appendix. Included with the standard testing data is modulus data generated by NIST Gaithersburg using a dynamic elastic modulus measurement technique.
   One of the main objectives of this quarter was to fatigue the pipeline specimen materials obtained from PG&E. We received the pipeline sections from PG&E and machined them into appropriately sized full-thickness fatigue specimens. The PG&E pipes are 20 to 25 in. in diameter and have wall thicknesses of 5/16" and 3/8". The specimens are oriented along the axis of the pipe length and the fatigue crack is transverse to the axial direction (hoop direction) of the pipe. The fatigue specimens are hourglass shaped and have a test section width of 4" and a reduced section length of 6". A ½" wide notch was electrical discharge machined in the center of the specimens as a starter for the fatigue pre-crack. The specimens were fatigue pre-cracked to a predetermined length and then fatigued while recording fatigue crack growth rate data. A sample of the FCGR data can also be seen in the attached appendix.

   Another focus during this period was to conduct Crack-Tip Opening Angle Testing (CTOA) on the supplied pipeline materials. CTOA, originally based on the COD ductile fracture criterion, has been proposed as a fracture parameter in linepipe steels as a measure of dynamic, ductile, and steady-state fracture toughness. CTOA specimens were machined from the pipeline sections with the notch and crack aligned with the axial direction of the pipes. The specimens were typically machined to be 3 mm thick because of the wall thickness and curvature of the pipe wall and a desire not to flatten the sections for testing. The specimens were 100mm wide and 200 mm long. A notch, 60 mm long from the load centerline, was machined in the front edge of the specimens to facilitate a 2-4 mm pre-crack. In addition, we machined one API-5L-X100 steel CTOA specimen with the notch oriented so that the crack will grow across the transition from base-metal to heat affected zone to weld metal and then back into the HAZ and base metal. This specimen should give us an idea as to the

ductile fracture characteristics of the weld metal/HAZ area. Sample test results from the fatigue and CTOA experiments are included in this report.

With Colorado School of Mines, we finished the Proceedings of the April 2004 Workshop on Coating Technology (held in Biloxi, Mississippi) and distributed copies to the attendees and key government program managers. In addition, we prepared compact discs of the proceedings of the June 2005 workshop on corrosion held in Gaithersburg, MD and distributed copies to all attendees and key government managers.

British Petroleum provided us with a previously tested full size pipe section of API-5L-X100. The pipe section is about 25 feet long, 52" diameter and has a wall thickness of slightly less than 1 inch. In addition to this section, they also sent us some fractured pieces from the tested pipe, and another section that was about 4 feet long with a diameter and wall thickness to match the above described pipe. We torch cut a number of pieces from this short section in order to make tensile, fatigue and CTOA specimens. We also sent a piece, approximately 2'X2', to Chris San Marchi of Sandia Livermore Labs, for his experiments on high pressure hydrogen testing. We also received some API-5L-X65 pipeline steels from BP in three different wall thicknesses and diameters.

We had two attendees at the October meeting of the PRCI held in Galveston, TX. While there, we had a number of helpful technical discussions and interactions with other attendees, affirming our research direction. We also discussed our proposed plan to conduct high rate CTOA tests on full-thickness pipeline specimens using equipment available at NIST-Boulder. This information, combined with the Kolsky testing in Gaithersburg, would be valuable for the strain based design of pipelines currently being funded by the PRCI and DOT. We were also able to promote the upcoming Welding Workshop to be held in Boulder in late January of 2006.

We also attended the Banff Workshop in April of this year and presented our work to date on the PG&E steels.

**1. Activities Planned for the Next Reporting Period:**

a). Task 2 Fatigue: We will continue our FCGR program, generating fatigue data for a database on pipeline steels. Included in this database will be FCGR data on the API-5L-X100 and the API-5L-X65 pipeline steels provided by BP.

b). Task 3 Crack Arrest: Our work on ductile fracture crack resistance will continue through our efforts in CTOA testing. We have completed the CTOA work on the PG&E steels and plan to continue work on the X65 and X100 grades of steel and the girth weld associated with the X100 pipe material. We will be conducting CTOA tests on a variety of thicknesses to measure the effects of thickness on this measurement technique.

c). Tasks 4-6 to follow initial fatigue work.

d). Meetings and Committee Activities: NIST will continue to support pipeline R&D community through participation in organization of meetings, standards committee activities, and through participation in the interagency PSIA coordinating committee. We plan to continue our attendance at the PRCI meetings and DOT workshops, enabling us to keep abreast of the most current needs of the pipeline community. We will be hosting the Welding Workshop in Boulder in January of 2006.

e). Future Work: After discussions with other pipeline researchers we found that there is a need for high rate CTOA testing on high strength pipeline steels. While the drop weight tear test is adequate for testing the ductile fracture properties of lower strength steels, it is inadequate for the high toughness, high strength pipeline steels proposed for use today. We plan to propose future work on the effects of high strain rate on high strength pipeline steels using CTOA. This type of dynamic testing will most likely simulate the actual running crack conditions seen in a pipeline undergoing ductile fracture.

# Appendix

## Mechanical properties

### Uni-axial tensile properties

Table 1 list some tensile properties as obtained by the uniaxial test for the various pipes. In addition to the standard values, the ratios of $\sigma_{0.2}/\sigma_{UTS}$ and $e_u/e_f$ are also given. These two parameters indicate the strain hardening potential of the steel. The highlighted numbers in the modulus column indicate the effect of the microcracking on the measured modulus derived from the stress-strain curve of the experimental test. The dynamic elastic modulus values (a more accurate method of modulus measurement) are shown in Table 2. As shown in figure 1, as the stress ratio increases, the strain ratio decreases, with a moderate trend for the T direction and a more steep trend for the L direction. The ratios of the various pipes are also given on the both L and T curves.

Table 1. Standard mechanical properties at L and T orientations for the tested pipes

| Pipe | No | Orientation | E GPa | $\sigma_{0.2}$ MPa | $\sigma_{UTS}$ MPa | $\sigma_{0.2}/\sigma_{UTS}$ | $e_u$ % | $e_f$ % | $e_u/e_f$ | Remarks |
|---|---|---|---|---|---|---|---|---|---|---|
| **1** | 1 | L | 215 | 520 | 615 | 0.85 | 7.2 | 34.8 | 0.2 | Unused pipe |
| | 2 | L | 205 | 510 | 608 | 0.84 | 7.2 | 35.1 | 0.2 | |
| | 1 | T | 221 | 555 | 603 | 0.92 | 8.6 | 27 | 0.31 | |
| | 2 | T | 227 | 535 | 609 | 0.88 | 8.8 | 27.7 | 0.32 | |
| **2** | 1 | L | **180** | 375 | 556 | 0.67 | 12.4 | 31.2 | 0.35 | X52 |
| | 2 | L | **175** | 360 | 557 | 0.65 | 12.8 | 34 | 0.37 | |
| | 1 | T | 207 | 460 | 573 | 0.80 | 10.2 | 25.6 | 0.40 | |
| | 2 | T | 216 | 445 | 578 | 0.77 | 10 | 25.5 | 0.39 | |
| **3** | 1 | L | **195** | 245 | 450 | 0.54 | 19.5 | 37.4 | 0.52 | GRB |
| | 2 | L | **195** | 245 | 451 | 0.54 | 19 | 38.2 | 0.5 | |
| | 1 | T | 202 | 260 | 460 | 0.56 | 20 | 38.7 | 0.52 | |
| | 2 | T | 197 | 255 | 458 | 0.56 | 19 | 37.3 | 0.51 | |
| **5** | 1 | L | **180** | 335 | 535 | 0.62 | 14 | 35.1 | 0.4 | No I.D. |
| | 2 | L | **181** | 335 | 536 | 0.62 | 13 | 34.7 | 0.38 | |
| | 1 | T | 207 | 425 | 559 | 0.76 | 9.6 | 21.9 | 0.44 | |
| | 2 | T | 205 | 427 | 561 | 0.76 | 9.4 | 22 | 0.43 | |
| **6** | 1 | L | 206 | 272 | 455 | 0.6 | 17.4 | 37.8 | 0.46 | ? |
| | 2 | L | 205 | 288 | 459 | 0.63 | 17.5 | 38.2 | 0.46 | |
| | 1 | T | 208 | 250 | 455 | 0.55 | 19 | 33 | 0.58 | |
| | 2 | T | 196 | 250 | 453 | 0.55 | 19.2 | 37 | 0.52 | |

The following modulus measurements were made according to ASTM E 1876, using a dynamic elastic modulus measurement technique. These measurements were made on machined samples, with all microcracking removed from the samples.

Table 2. Dynamic modulus measurements on pipeline steels

| Sample No. | Meas Date | E(1) | E(2) | E(4) | G(3) | μ |
|---|---|---|---|---|---|---|
| 1 | 3/30/2005 | 212 | 210 | 211 | 82 | 0.284 |
| 2 | 3/30/2005 | 210 | 212 | 209 | 81 | 0.294 |
| 3 | 3/30/2005 | 213 | 211 | 211 | 82 | 0.287 |
| 4 | | | | | | |
| 5 | 3/30/2005 | 210 | 211 | 209 | 82 | 0.284 |
| 6 | 3/30/2005 | 214 | 214 | 212 | 82 | 0.294 |
| | Mean | 212 | 212.6 | 211.1 | 82.5 | 0.289 |
| | Std Dev | 2.2 | 1.8 | 1.3 | 0.4 | 0.005 |

| | | |
|---|---|---|
| Mean E(all) | 212 | Adiabatic |
| Std Dev | 1.24 | |
| Est Isothermal | | |
| E | 207.5 | Isothermal |
| ± | 1.24 | |

E(1)= Measured for out-of-plane flexure which has the greatest strains on the wide flat sides
E(2)= Measured for in-plane flexure which has the greatest strains on the long edges.
E(4)= Measured for longitudinal vibrations with equal strains across cross section.
G(3)= Shear modulus measured in torsion bending mode.

Note: All E measurements are in the long dimension of the sample.
Note: For 6.35 mm (1/4 in) thick steel the adiabatic to isothermal transition loading freq is about 1 Hz.

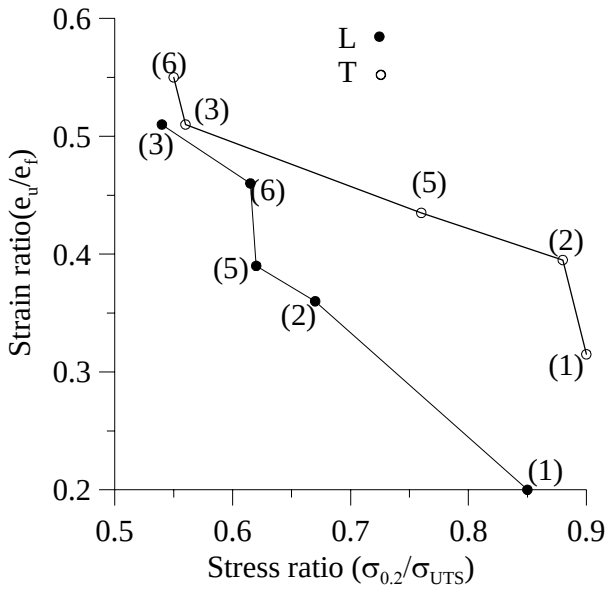


Figure 1. The dependency of the strain ratio with the stress ratio for both orientations.

Figures 2a and b summarize the values of the yield and the ultimate stresses in decreasing order for both directions and the appropriate uniform and total elongation respectively. As shown, pipe 1 exhibits the higher stresses with the lowest uniform elongation for the both directions. However, the lowest value for the total elongation was observed for pipe 5. Pipe 3 displays the lowest stresses with the highest uniform and total elongation. The most inconsistent trend for the total elongation in the T orientation for the uniform elongation was seen for pipe 2 and 5. This behavior is attributed to the preferred orientation, evident in the microstructure.

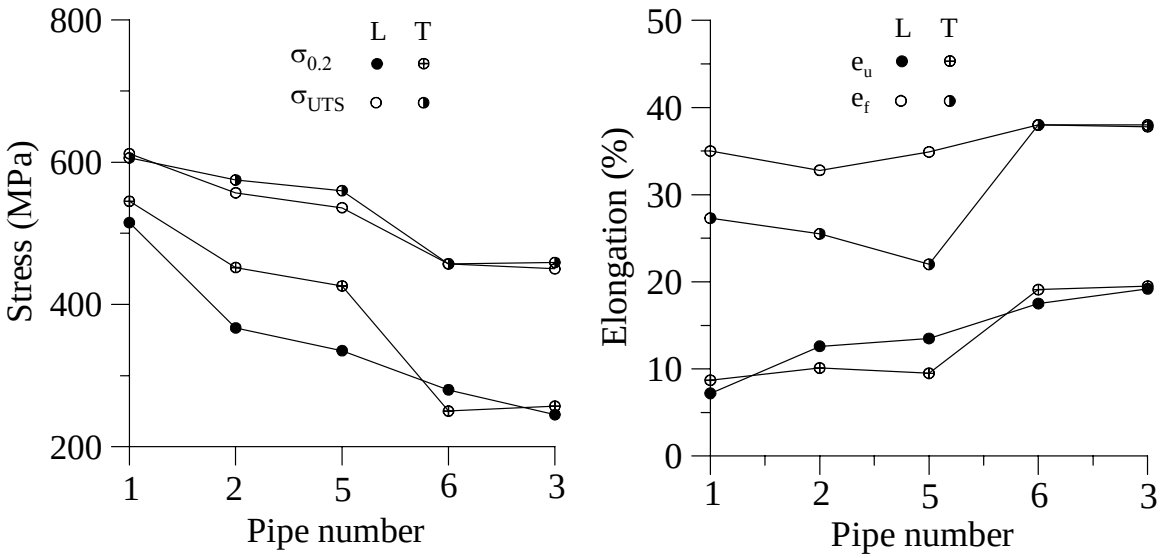


Figure 2. The highest through lowest yield and ultimate stress for both directions (a), and the respectively uniform and the total elongation (b).

The low Young's modulus (highlighted) obtained for pipes 2, 3 and 5 is attributed to the global damage of microcracking at the interior and exterior surfaces of the pipe due to the corrosion and stress corrosion cracking processes. Selected figures 3a,-d demonstrate such damage for the mentioned pipes. In pipe 3 (figures 8b-d) some crack–like features at the corrosion front and some areas that likely reflect corrosion within pearlite colonies were noticed more than in other pipes. In this pipe, it was not apparent that MnS stringers were preferred corrosion sites near the front.

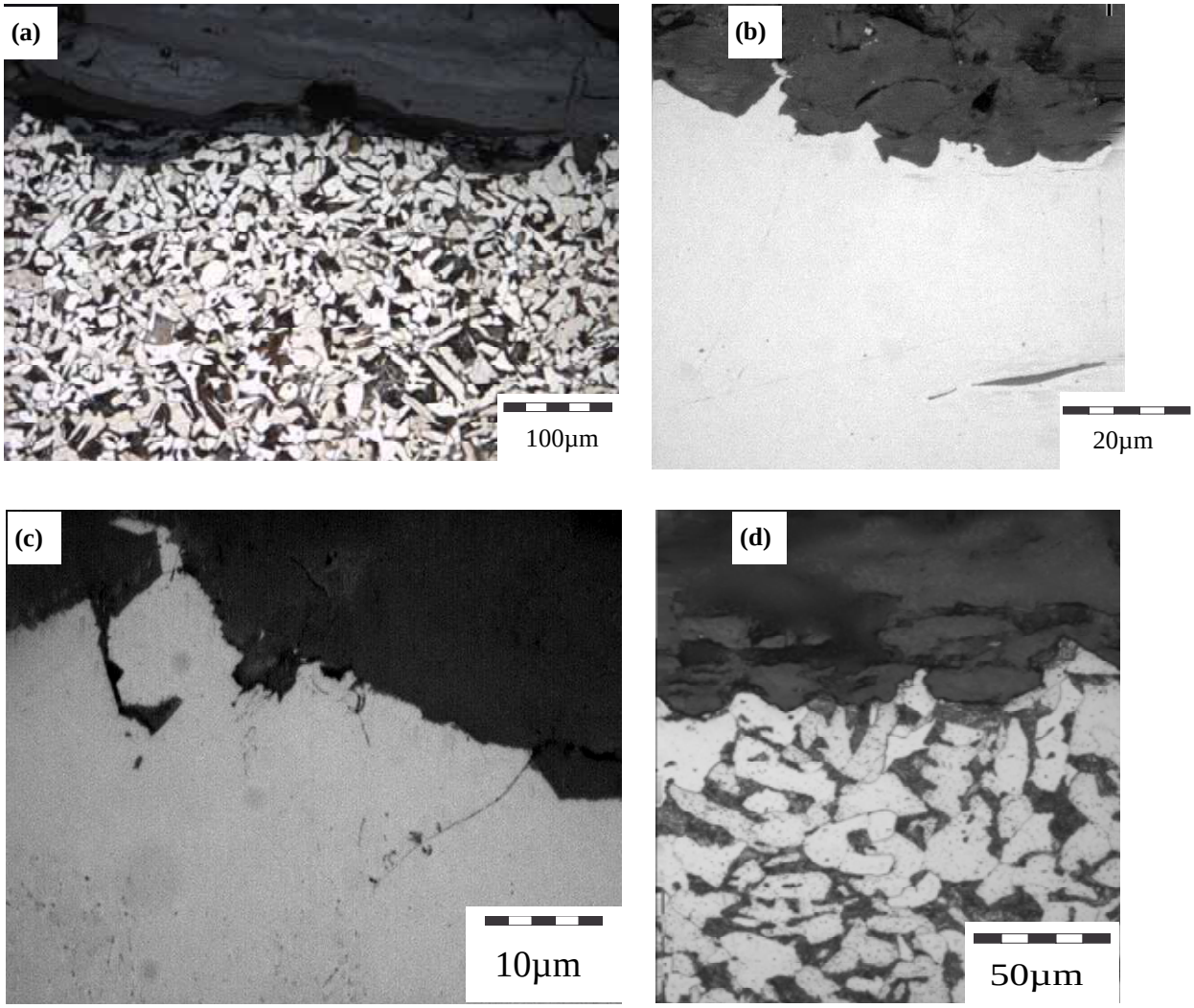


Figure 3. The corrosion and stress corrosion cracking in uniform general manners in selected pipes, (a) pipe 2, (c-b) pipe 3 , (d) pipe 5.

Although the original thickness is almost unaffected, the surface's which were damaged by the corrosion process exhibits microcracking while being stretched during the tensile test. In turn, this decreases the effective cross section, which affects the elastic slope. Thus, the ratio of the damaged E to the undamaged E can qualitatively point out the degree of damage.

Figure 4 depicted typical stress-strain behavior curve for the tested pipes for both directions. As shown, pipe 5 exhibits the highest degree of preferred orientation as reflected by the microstructure. Pipe 3 displays almost no preferred directional property which is also supported by the uniform microstructure.

Figure 5a and b compare the plastic flow region for the tested pipes in both orientations. In the T orientation, the changes in the plastic flow behavior are more noticeable as compared to the L orientation. As mentioned, the banded ferrite-pearlite and the inclusions content are the moresignificant factors in influencing the strain hardening potential.

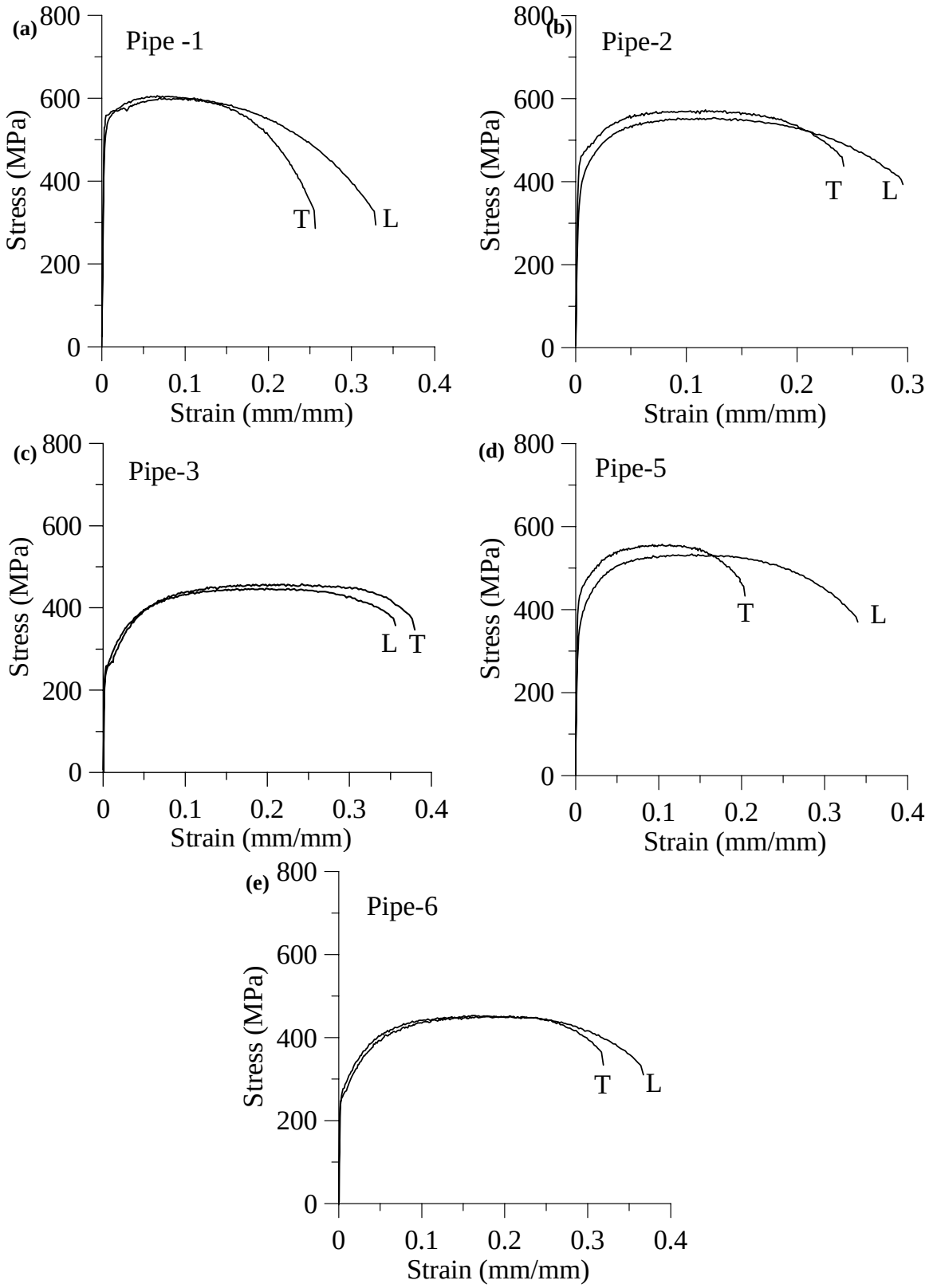


Figure 4. Stress-strain curves for the tested pipes in longitudinal and transverse orientations.

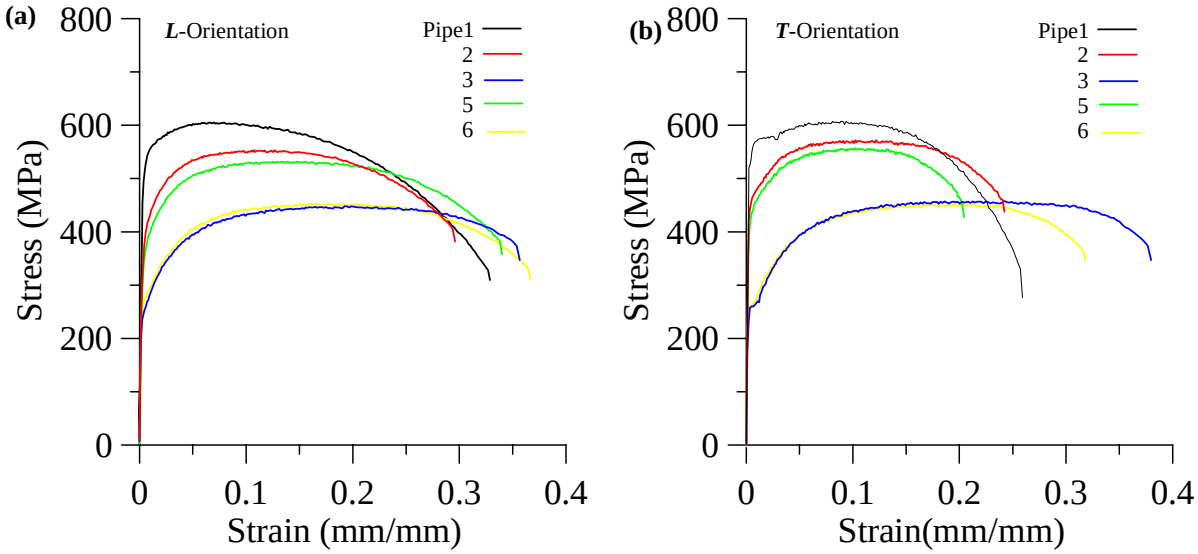


Figure 5. Comparison of the plastic flow for the various pipes as a function of orientation (a) L, (b) T.

Typical fatigue crack propagation results are shown in figure 6a and b for pipeline 2. This data compares well with published data from literature (Vosikovsky). Figure 7 and 8 show the macro fatigue fracture surfaces of the curved pipeline sections. The fatigue specimens were removed from the pipe and all fatigue cracks were initiated from electrical discharged machined center notches and propagated transverse to the pipeline longitudinal axis.

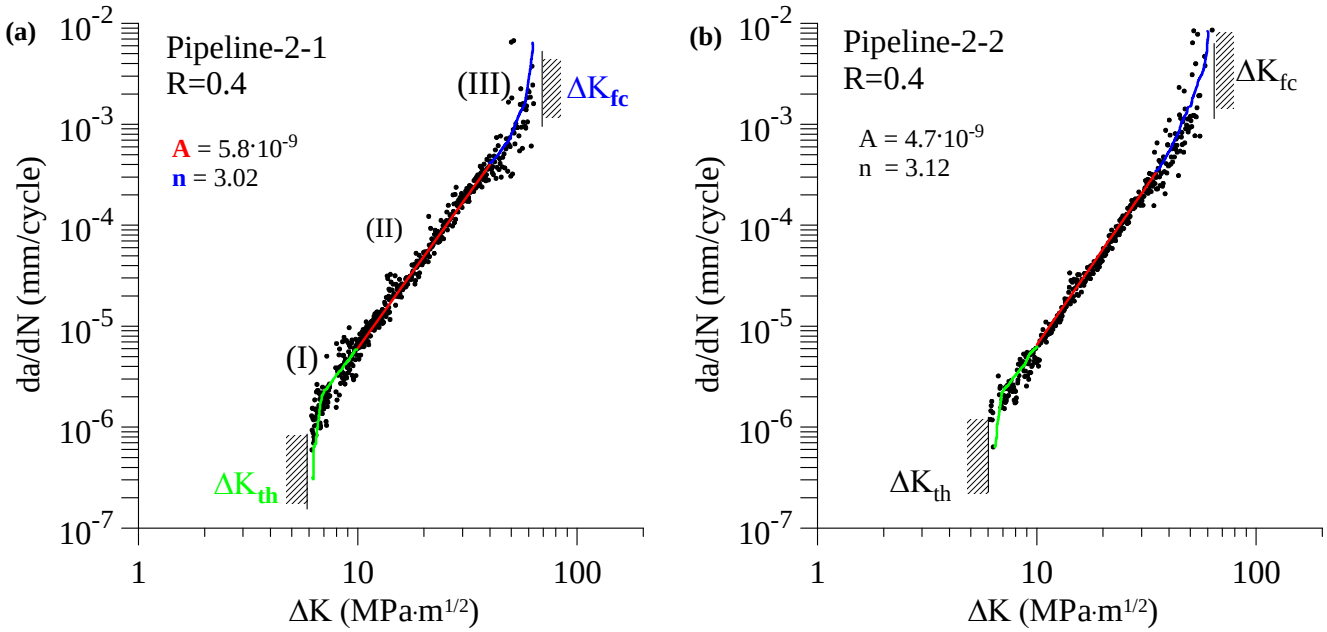


Figure 6 Fatigue crack propagation rate curves for pipeline 2 (a) spec. 1, (b) spec. 2.

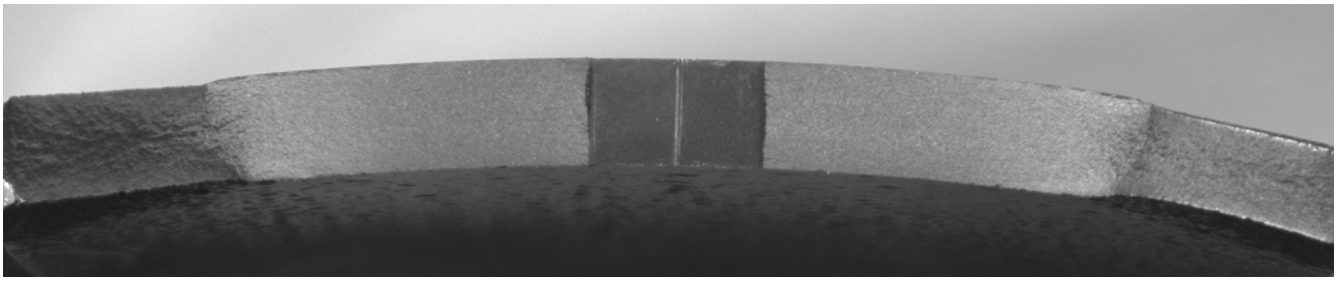

Figure 7. Macro fatigue fracture with emphasis on the symetrical crack front with some deviation at the later stage of fatigue crack growth.

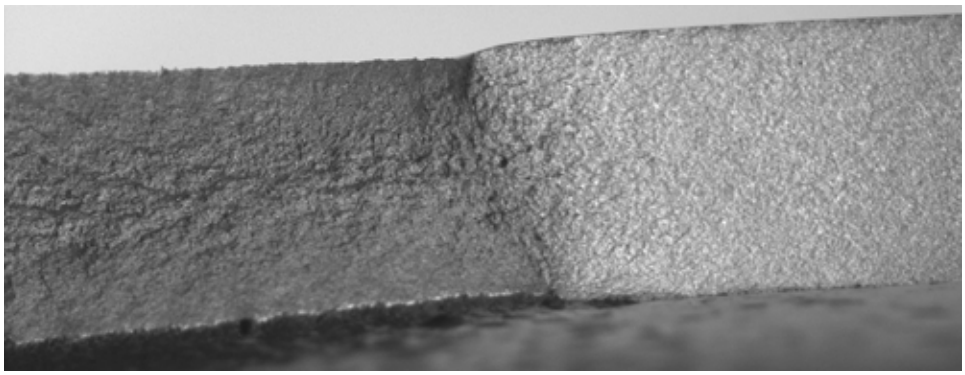

Figure 8. Macro fatigue fracture at the later stage accompanied by shear fracture mode resulting from monotonic loading.

## CTOA results

## Pipeline 1.

Figures 9a and 9b illustrate the CTOA curve profile with the crack extension. As shown there is a steep change of the CTOA value at the initial crack growth followed by a moderate change up to 5mm. From this point a stable CTOA was observed which actually characterized the critical CTOA, a material property similar to the fracture toughness parameter. Note the larger value of CTOA obtained while using all the images pictures (figure 9a) as compare to the one obtained while using every tenth image (figure 9b). Figure 10 depicts the load-COD curve obtained during the CTOA test, accompanied by selected crack tip contour at different load level. As can be observed, progressive crack tip blunting occurs up to nearly the maximum load. Then crack initiation takes place followed by crack growth with almost no change in the load. This crack extension region is dominated by the normal stress field, which is reflected by ductile flat fracture mode (see figure 11a). This crack growth stage is followed by mixed mode crack growth, normally with shear (the dashed area limited by shear zones –figure 11b). This type of crack growth was accompanied by a slight decrease in load , then a full shear crack growth occurred (see figure 11b) (related to the stable CTOA) with a moderate decrease in load.

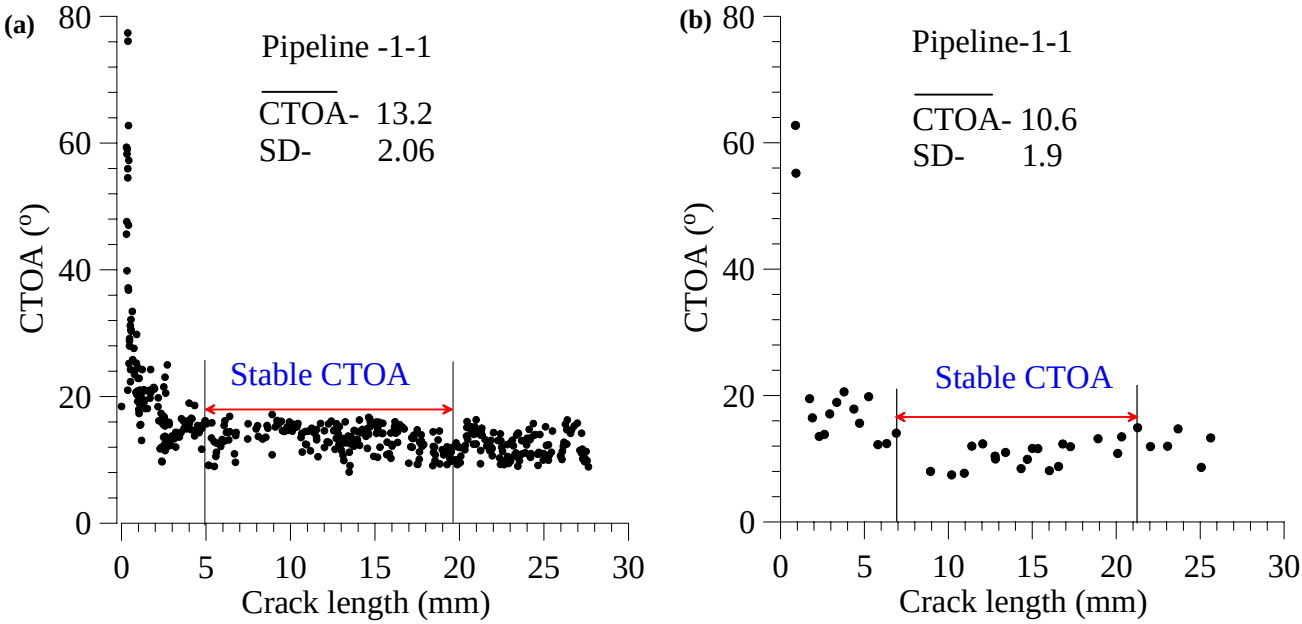


Figure 9. Mean CTOA value determined by using; (a) all the pictures, (b) every 10 pictures.

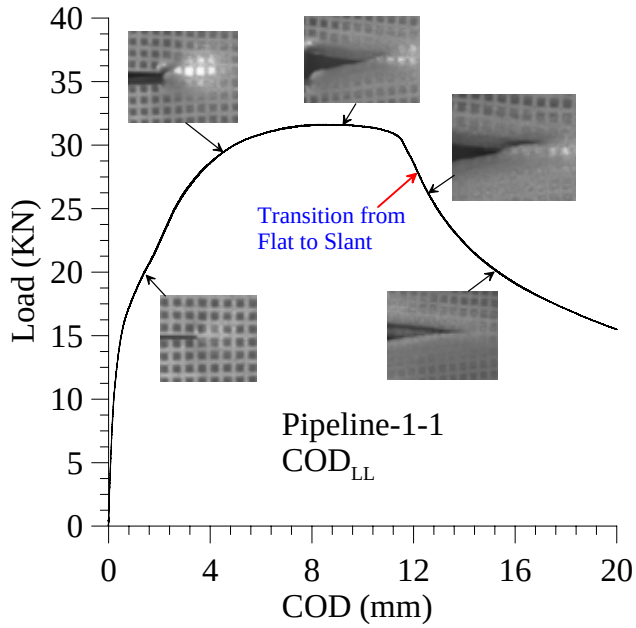


Figure 10. Load vs $COD_{LL}$ curve and the change of crack tip profile during crack growth with loading. LL indicates that the COD gage was mounted at the load line

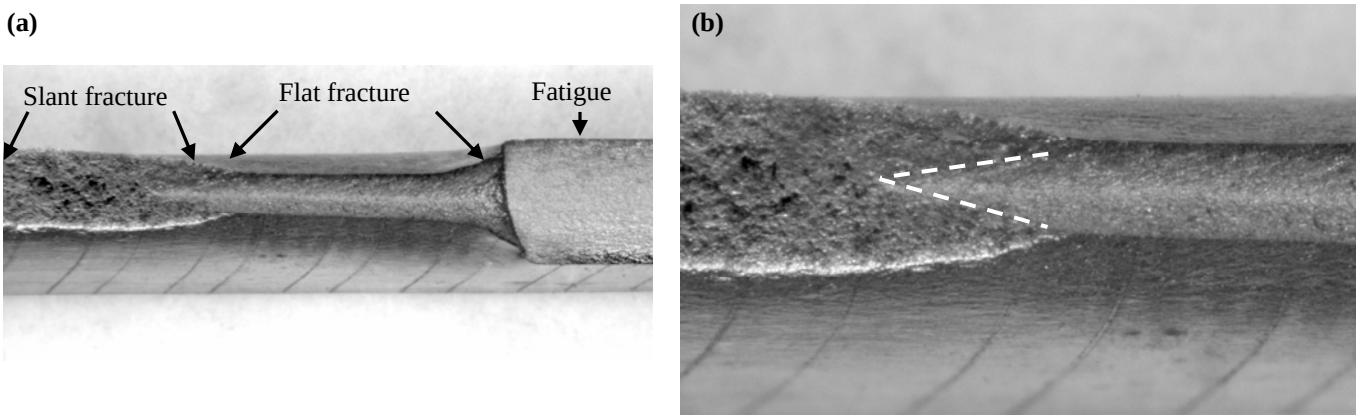


Figure 11. Macro fracture surface of a CTOA specimen indicating the transition from flat to slant fracture , (a) the various modes fracture, fatigue flat and slant, (b) and the transition fracture area.